ON THE USE OF BEAMFORMING FOR ESTIMATION OF SPATIALLY DISTRIBUTED SIGNALS

*Mikael Tapio**

Department of Signals & Systems
Chalmers University of Technology, SWEDEN
mito@s2.chalmers.se

ABSTRACT

In wireless communications, spatially distributed signals originate from local scattering around the transmitter. Spatially distributed signals cause conventional high-resolution methods to show degradation in performance, since the underlying data model is of full rank theoretically. In this paper, a relationship between the distribution of the spatial spread and the Power Azimuth Spectrum is derived. Using this relationship, two simple and robust estimators based on the conventional beamformer and Capon's beamformer for estimation of the nominal direction and spatial spread are found. The proposed estimators show very good performance in numerical examples.

1. INTRODUCTION

Many classical Direction Of Arrival (DOA) estimation methods are based on point source models. In some cases, for example, in indoor radio communications, the point source assumption is violated, and a distributed source model would be a better approximation [8]. Another example is fast fading in mobile communications, where the elevated base-station antenna, due to local scattering around the mobile, experiences the received signal as distributed in space rather than being emitted from a point source [12]. In conventional high-resolution DOA estimation methods this leads to deterioration in performance, and therefore a number of high-resolution estimators for distributed sources have recently been proposed, e.g. [2, 3, 5, 9, 10]. Many of these estimators make assumptions on the shape of the signal distribution, assume narrow spatial spreads, and eigen-decompose the full-rank covariance matrix into a pseudo-signal subspace and a pseudo-noise subspace. Most often they render a multi-dimensional optimization problem, implying high computational loads.

In many applications, e.g. fast fading mobile communications, wireless indoor communications etc., we know little or nothing about the spatial distribution of the signals. Therefore, it would be attractive to make use of a robust and simple beamformer that does not make any assumptions on signal distribution nor uses any hard-to-choose design parameters.

In this paper, the work in [7] is extended and the resulting estimator performance is dramatically improved. We first derive a relationship between the Power Azimuth Spectrum (PAS) and the underlying distribution of the scattered source signal. The result enables the use of simple beamforming-based techniques for localization and spread estimation of a distributed signal. Numerical examples show that the proposed estimators perform very well.

*This work was supported in part by the Personal Computing and Communication Program (PCC++). PCC++ is funded by the Swedish Foundation for Strategic Research.

2. DISTRIBUTED SIGNAL MODEL

We use the distributed signal model suggested in [1], in which the distributed signal impinging upon a Uniform Linear Array (ULA) is modeled as being emitted from a tight cluster of L spatially separated point sources (or scatterers), each with random complex gains. Thus, the received signal can be written as

$$\mathbf{x}(t) \quad = \quad s(t) \sum_{\ell=1}^{L} \gamma_\ell(t) \mathbf{a}(\theta_0 + \tilde{\theta}_\ell(t)) + \mathbf{n}(t) \ , \qquad (1)$$

where $\gamma_\ell(t)$, θ_0, and $\tilde{\theta}_\ell(t)$, are, respectively, the complex gain of ray ℓ, nominal (or mean) DOA, and random spatial (angular) deviation of ray ℓ. The K-sensor array steering vector is denoted by $\mathbf{a}(\theta) = [1, e^{-jkd\sin\theta}, \ldots, e^{-j(K-1)kd\sin\theta}]^T$, where $k = 2\pi/\lambda$ (wavelength – λ) denotes the circular wave number, and d is the element separation. Finally, $s(t)$ denotes the transmitted source signal, and $\mathbf{n}(t)$ the noise, which is modeled as a zero-mean complex circularly symmetric, and spatio-temporally white Gaussian process with variance σ^2.

As in [1, 9], it is also assumed that the scattering environment changes rapidly compared to the mean DOA and spread parameters, i.e. the random complex gains $\gamma_\ell(t)$ are assumed to be temporally white. Further, they are also assumed to be independent from ray to ray, zero-mean, and circularly symmetric

$$E\left[\gamma_\ell(t)\right] = 0 \ , \qquad E\left[\gamma_\ell(t)\gamma_k(s)\right] = 0 \ ,$$
$$E\left[\gamma_\ell(t)\gamma_k^*(s)\right] = \frac{1}{L}\sigma_\gamma^2 \delta_{\ell k}\delta_{ts} \ , \quad \forall\ \ell, k, t, s \ , \qquad (2)$$

where $\delta_{\ell k}$ is the Kronecker delta function.

The random spatial deviation $\tilde{\theta}_\ell(t)$ is assumed to be a zero-mean random variable described by a Probability Density Function (PDF) $p(\tilde{\theta}; \sigma_\theta)$. The PDF is assumed to be symmetric in $\tilde{\theta}$ and parameterized by a spread (or standard deviation) parameter σ_θ. Note that the resulting estimators do not require a symmetric PDF.

By assuming large L, and using the central limit theorem, it is argued in [1, 9] that $\mathbf{x}(t)$ is a zero-mean complex Gaussian vector with covariance matrix

$$\begin{aligned}
\mathbf{R}_x &= E\left[\mathbf{x}(t)\mathbf{x}^H(t)\right] \\
&= E_{\tilde{\theta}}\left[\, E\left[\mathbf{x}(t)\mathbf{x}^H(t) \,\middle|\, \tilde{\theta}\right]\right] \\
&= \sigma_s^2\sigma_\gamma^2 \int_{\tilde{\theta}} p(\tilde{\theta}; \sigma_\theta)\mathbf{a}(\theta_0 + \tilde{\theta})\mathbf{a}^H(\theta_0 + \tilde{\theta}) d\tilde{\theta} + \sigma^2\mathbf{I} \\
&= S\mathbf{R}_v(\theta_0, \sigma_\theta) + \sigma^2\mathbf{I} \ , \qquad (3)
\end{aligned}$$

where $S = \sigma_s^2\sigma_\gamma^2 = E[|s(t)|^2]\sigma_\gamma^2$ is the source signal power including the path gain factor, and $\mathbf{R}_v(\theta_0, \sigma_\theta)$ is the channel covariance matrix (excluding the path gain) of the zero-mean Gaussian channel vectors. In the limit, the cluster of scatterers can be viewed upon as a continuum of scatterers, i.e. the spatio-temporal complex gain can be described by a temporal stochastic process $\gamma(\tilde{\theta}; t)$, which has a continuous spatial distribution with covariance kernel $E\big[\gamma(\tilde{\theta}_1; t)\gamma^*(\tilde{\theta}_2; t)\big] = \sigma_\gamma^2 p(\tilde{\theta}_1; \sigma_\theta)\delta(\tilde{\theta}_1 - \tilde{\theta}_2)$. In this context, $p(\tilde{\theta}; \sigma_\theta)$ can be viewed upon as a continuous *Spatial Power Density Function (SPDF)*.

The spatial deviation is commonly modeled by a Gaussian distribution, i.e. $\tilde{\theta} \sim \mathcal{N}(0, \sigma_\theta)$. For small Gaussian spatial spreads, the $(m, n)^{\text{th}}$ entry of the covariance matrix can be written as [1, 2]

$$[\mathbf{R}_v(\omega_0, \sigma_\omega)]_{m,n} = \exp(j(m-n)\omega_0) \times \exp(-0.5((m-n)\sigma_\omega)^2), \quad (4)$$

where $\omega_0 = kd\sin\theta_0$ denotes the *spatial frequency*, and $\sigma_\omega = kd\sigma_\theta\cos\theta_0$ denotes corresponding standard deviation.

3. BEAMFORMING-BASED ESTIMATION

The DOA of a single deterministic point source is usually taken as the peak of the Power Azimuth Spectrum (PAS)

$$\hat{\theta} = \arg\max_\theta \hat{P}(\theta) \ , \quad (5)$$

where $\hat{P}(\theta)$ denotes the estimated PAS, from the sample covariance matrix. Using the true covariance matrix, the PAS is given by

$$P(\theta) = \begin{cases} \frac{\mathbf{a}^H(\theta)\mathbf{R}_x\mathbf{a}(\theta)}{\mathbf{a}^H(\theta)\mathbf{a}(\theta)} & -\text{CBF} \\ \frac{1}{\mathbf{a}^H(\theta)\mathbf{R}_x^{-1}\mathbf{a}(\theta)} & -\text{Capon.} \end{cases} \quad (6)$$

Capon's beamformer [4] has higher resolution than the Conventional Beamformer (CBF). This is achieved at the expense of reduced white noise suppression. The performance of CBF for distributed sources was analyzed in [6], where the nominal DOA estimate was taken from Eqn. (5). In general, the performance of the peak-finding algorithm is poor for distributed sources.

Assume that the steering vectors corresponding to distinct directions are orthogonal for large K, i.e.

$$\lim_{K\to\infty} \frac{1}{K}\mathbf{a}^H(\theta)\mathbf{a}(\eta) = \begin{cases} 1 \ , & \theta = \eta \\ 0 \ , & \theta \neq \eta. \end{cases} \quad (7)$$

Hence, for large K we have $\frac{1}{K}\mathbf{A}^H(\boldsymbol{\theta})\mathbf{A}(\boldsymbol{\theta}) \approx \mathbf{I}$, where $\mathbf{A}(\boldsymbol{\theta})$ denotes the $K \times L$ steering matrix of the vector $\boldsymbol{\theta} = [\theta_1, \ldots, \theta_L]^T$.

The discrete version of the covariance matrix in (3) can be written $\mathbf{R}_v = \sum_{\ell=1}^L p(\theta_\ell)\mathbf{a}(\theta_\ell)\mathbf{a}^H(\theta_\ell) = \mathbf{A}(\boldsymbol{\theta})\mathbf{P}(\boldsymbol{\theta})\mathbf{A}^H(\boldsymbol{\theta})$, where $\mathbf{P}(\boldsymbol{\theta})$ denotes a diagonal matrix with the power mass entries $[\mathbf{P}(\boldsymbol{\theta})]_{\ell,\ell} = p(\theta_\ell)$. Since it is only non-zero values of $p(\theta_\ell)$ that contribute to the channel covariance matrix, we let $p(\theta_\ell) > 0$ to make $\mathbf{P}$ full rank. Note that in this context, θ_ℓ is equal to the nominal DOA θ_0 plus the previously used random deviation $\tilde{\theta}_\ell$ of ray ℓ.

Using the matrix inversion lemma and assuming large K, the inverse covariance matrix becomes $\mathbf{R}_x^{-1} = [S\mathbf{R}_v + \sigma^2\mathbf{I}]^{-1} = [S\mathbf{A}\check{\mathbf{P}}\mathbf{A}^H + \sigma^2\mathbf{I}]^{-1} \approx \mathbf{A}\check{\mathbf{P}}\mathbf{A}^H + \sigma^{-2}\mathbf{I}$, where $\check{\mathbf{P}}$ is the diagonal matrix with entries $[\check{\mathbf{P}}]_{\ell,\ell} = -\frac{Sp(\theta_\ell)}{\sigma^4 + \sigma^2 SKp(\theta_\ell)}$. It is now straightforward to insert $\mathbf{R}_x$ and $\mathbf{R}_x^{-1}$ into the expressions for the PAS given by Eqn. (6). Doing so, we find the following relationship

$$P(\theta_\ell) \approx \beta p(\theta_\ell; \theta_0, \sigma_\theta) + \varepsilon \ , \quad \beta \geq 0, \ \varepsilon \geq 0 \ , \quad (8)$$

where $\beta = SK$, $\varepsilon = \sigma^2$ for the CBF spectrum, and $\beta = S$, $\varepsilon = \frac{\sigma^2}{K}$ for Capon's spectrum.

Now, to find our parameters $\{\theta_0, \sigma_\theta\}$ we have to decide the support Ω of the underlying PDF. Also, since the underlying PDF does not necessarily have a finite support (e.g. Gaussian PDF), we have to restrict the support to be finite. For example, the support of a Gaussian PDF with mean θ_0 and standard deviation σ_θ can with negligible error be restricted to $[\theta_0 - 3\sigma_\theta, \theta_0 + 3\sigma_\theta] \subset (-90^\circ, 90^\circ)$. The obvious problem that arises here is how to choose the support. One criterion for choosing it is to find the region where the signal part of the PAS is distinct from the noise power level. The best would of course be if we could find the interval from data, but for now it is left as an open problem.

When we have decided the support Ω, the scaling factor β is easily found. We simply subtract the minimum value of $P(\theta)$ on Ω, which corresponds to ε, from $P(\theta)$. Then we use the fact that $p(\theta_\ell; \theta_0, \sigma_\theta)$ is a PDF (or rather a probability mass function) and should therefore sum to unity, i.e. β can be found as $\beta = \sum_{\theta_\ell\in\Omega}\tilde{P}(\theta_\ell)$, where $\tilde{P}(\theta) = P(\theta) - \min_{\theta\in\Omega}P(\theta)$ and is positive semi-definite.

Putting it all together and using the standard definitions of mean value and standard deviation, the nominal DOA actually becomes the Center of Mass (CM) of $\tilde{P}(\theta)$ on Ω

$$\theta_0 = \frac{\sum_{\theta_\ell\in\Omega}\theta_\ell\tilde{P}(\theta_\ell)}{\sum_{\theta_\ell\in\Omega}\tilde{P}(\theta_\ell)} \ , \quad (9)$$

and the spatial spread parameter or standard deviation is given by

$$\sigma_\theta = \left(\frac{\sum_{\theta_\ell\in\Omega}(\theta_\ell - \hat{\theta}_0)^2\tilde{P}(\theta_\ell)}{\sum_{\theta_\ell\in\Omega}\tilde{P}(\theta_\ell)}\right)^{1/2} . \quad (10)$$

As mentioned earlier, when $L \to \infty$, the distributed source can be described by a continuous SPDF. Consequently, if we compute the PAS densely enough, the SPDF can be acquired from the PAS. It should also be mentioned that there is no requirement for the SPDF to be symmetric.

Finally, since the true covariance matrix $\mathbf{R}_x$ is unknown, we have to use the sample covariance matrix which is defined as $\hat{\mathbf{R}}_x = \frac{1}{N}\sum_{t=1}^N \mathbf{x}(t)\mathbf{x}^H(t)$ to estimate the PAS. It is well known [11] that $\hat{\mathbf{R}}_x$ converges (with probability one) to $\mathbf{R}_x$ as $N \to \infty$. Hence, the estimated PAS is a consistent estimate of the true PAS, and our estimate of $p(\theta; \theta_0, \sigma_\theta)$ becomes consistent, thus leading to consistent estimates of the nominal DOA and spread parameters. Note that we have used the assumption of orthogonal steering vectors. If the number of sensors is too small, the estimate of σ_θ will deteriorate.

Fig. 1 illustrates $\tilde{P}(\theta)/\beta$ for the CBF and Capon spectra when the theoretical angular distribution is Gaussian. Also included are Non-Linear Least Squares (NLLS) curve fits of $\beta p(\theta; \theta_0, \sigma_\theta) + \varepsilon$ (where $p(\theta; \theta_0, \sigma_\theta)$ is a Gaussian PDF) to the PAS. The NLLS problem is optimized over all four parameters but since it is linear in β and ε it can be separated and therefore a two-dimensional search is needed to find θ_0 and σ_θ. Both of the spectral-based PDF estimates $\tilde{P}(\theta)/\beta$ show good fit to the underlying Gaussian PDF and motivate the relationship given by Eqn. (8). Note that the NLLS fits are slightly worse than their corresponding PDF estimates. The support for the CBF and Capon estimates is limited to $\Omega = [\theta_0 - 3\sigma_\theta, \theta_0 + 3\sigma_\theta]$ which causes a better fit than their corresponding NLLS fits.

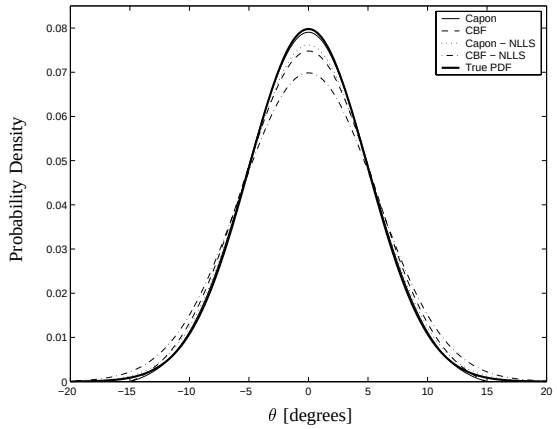

Fig. 1. Estimated PDFs. Gaussian spread, $\theta_0 = 0^\circ$, $\sigma_\theta = 5^\circ$, 18 sensors, theoretical covariance matrix with $S/\sigma^2 = 10$ dB.

4. NUMERICAL EXAMPLES

In this section simulations are presented to illustrate the performance of the different beamforming-based techniques for one Gaussian distributed source ($\theta_0 = 0^\circ$, $\sigma_\theta = 5^\circ$) versus the more complex subspace-based DISPARE [5] and WPSF [1, 3] algorithms. WPSF is not a very practical algorithm but serves as a bound on how well any low-rank approximation-based algorithm can perform. The Cramér-Rao Lower Bound (CRLB) and NLLS curve fits based on the Capon spectrum are also included in the figures for reference. Unless otherwise stated, an eight-element ULA with half-wavelength element separation is used. The received signal is generated from the model given by Eqn. (1), with $L = 100$ random DOAs and complex Gaussian gains $\gamma_\ell(t)$, and with a new independent realization for each snapshot. The source signal is an equiprobable BPSK sequence. The sample covariance matrix is computed over 100 independent channel realizations (snapshots). The DISPARE and WPSF estimates are acquired by letting the dimension, D, (design parameter) of the pseudo-signal subspace be such that it contains at least of 95% of the signal energy. To locate the solutions, a two-dimensional Nelder-Mead simplex search, initialized at the true parameter values, is used. We also let DISPARE and WPSF use the correct assumption that the deviation is Gaussian distributed. Again the support of the Capon and CBF estimates is limited to $\Omega = [\theta_0 - 3\sigma_\theta, \theta_0 + 3\sigma_\theta]$. Since the estimate of θ_0 is taken as the CM of the spectrum, it is not that sensitive to the choice of Ω. Clearly the spread estimate becomes more sensitive to the width of the interval Ω. The PASs are computed with a resolution of 0.1°.

Figs. 2 and 3 show the Root Mean Square Error (RMSE) of the estimated parameters $\hat{\theta}_0$ and $\hat{\sigma}_\theta$ versus SNR, respectively. Figs. 4 and 5 show the RMSE of estimated DOA and spread versus true spread σ_θ for 10 dB SNR. Finally, Figs. 6 and 7 show the RMSE of estimated DOA and spread versus number of sensors for 10 dB SNR. The RMSE is computed over 1000 independent trials for each parameter.

We see that it is better to choose the CM instead of the peak when estimating the nominal DOA. Capon show very good performance when estimating both the nominal DOA and spread, while CBF suffers from resolution problems. It is worth noting that the RMSE of the spread estimate is below the CRLB for low SNRs (15 dB and less). This is possible because information about the support Ω is incorperated into the estimators but is not captured by the CRLB. This is typically showing at low SNRs.

For increasing spread, DISPARE shows deterioration which is probably caused by a bad choice of D while WPSF and beamforming are less sensitive to an increasing spread. Also note that the resolution problem of the CBF is overcome for increasing spread. For the same reason as shortly discussed above, Capon's spread estimates are again below CRLB (SNR is 10 dB).

Finally, as one might expect, when taking the CM, the performance increases as the number of sensors increases. This is not the case when we take the peak value. Note that the CBF spread estimates become significantly better for increasing number of sensors, which is due to higher resolution capability. The Capon spread estimates are again below CRLB for small numbers of sensors and low SNR (10 dB).

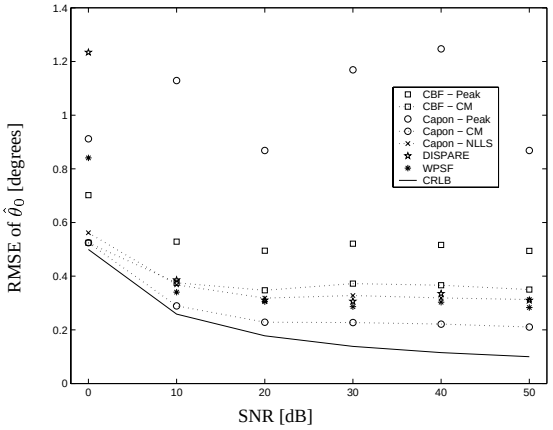

Fig. 2. RMSE of $\hat{\theta}_0$ for different SNRs. Gaussian spread, $\theta_0 = 0^\circ$, $\sigma_\theta = 5^\circ$, eight sensors, 100 scatterers.

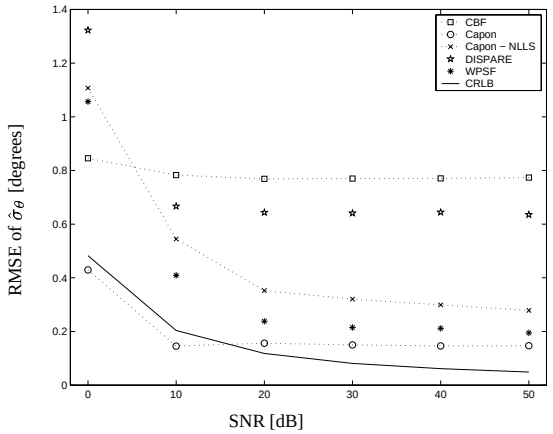

Fig. 3. RMSE of $\hat{\sigma}_\theta$ for different SNRs. Gaussian spread, $\theta_0 = 0^\circ$, $\sigma_\theta = 5^\circ$, eight sensors, 100 scatterers.

5. CONCLUSIONS

We have investigated the use of simple beamforming-based techniques to estimate the nominal DOA and spatial spread of a distributed signal. A relationship between the PAS and the underlying PDF was derived and from that result we found our estimators. The beamforming-based estimators showed very good performance and the estimators based on the Capon spectrum outperformed the two subspace-based estimators that were used in the

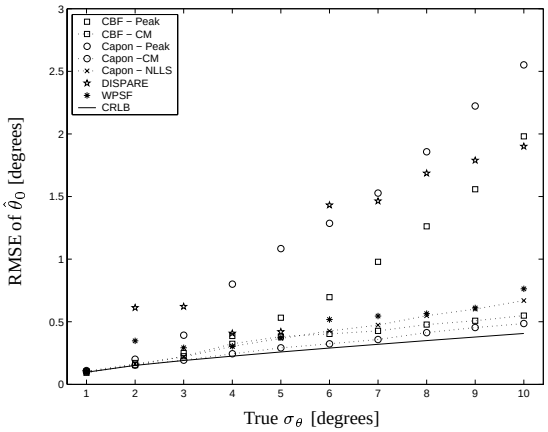

Fig. 4. RMSE of $\hat{\theta}_0$ for different spreads σ_θ. Gaussian spread, $\theta_0 = 0^\circ$, eight sensors, 100 scatterers, 10 dB SNR.

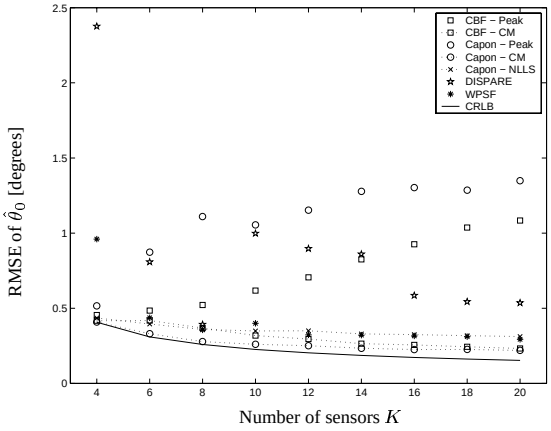

Fig. 6. RMSE of $\hat{\theta}_0$ for different numbers of sensors K. Gaussian spread, $\theta_0 = 0^\circ$, $\sigma_\theta = 5^\circ$, 100 scatterers, 10 dB SNR.

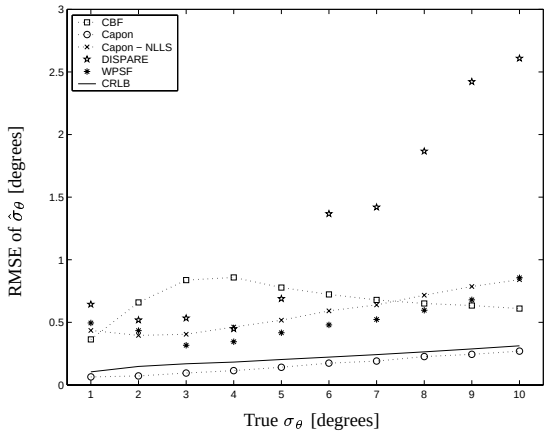

Fig. 5. RMSE of $\hat{\sigma}_\theta$ for different spreads σ_θ. Gaussian spread, $\theta_0 = 0^\circ$, eight sensors, 100 scatterers, 10 dB SNR.

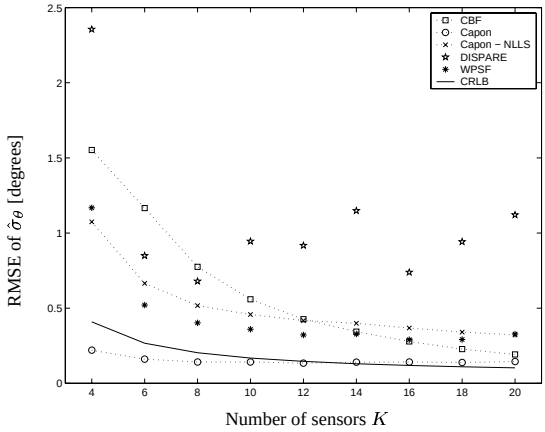

Fig. 7. RMSE of $\hat{\sigma}_\theta$ for different numbers of sensors K. Gaussian spread, $\theta_0 = 0^\circ$, $\sigma_\theta = 5^\circ$, 100 scatterers, 10 dB SNR.

numerical examples. One open problem remains and that is how to choose the support or decide on the interval of the signal part of the PAS. If the chosen support is too large, the spread estimate will deteriorate. The nominal DOA estimate is less sensitive to the choice of support.

6. REFERENCES

[1] M. Bengtsson. *"Antenna Array Signal Processing for High Rank Data Models"*. PhD thesis, Royal Institute of Technology, Stockholm, Sweden, 1999.

[2] M. Bengtsson and B. Ottersten. "Low-Complexity Estimators for Distributed Sources". *IEEE Trans. on Signal Processing*, 48(8):2185–2194, August 2000.

[3] M. Bengtsson and B. Ottersten. "A Generalization of Weighted Subspace Fitting to Full-Rank Models". *IEEE Trans. on Signal Processing*, 49(5):1002–1012, May 2001.

[4] J. Capon. "High Resolution Frequency Wave Number Spectrum Analysis". *In Proc. IEEE*, 57:1408–1418, 1969.

[5] Y. Meng, P. Stoica, and K.M. Wong. "Estimation of the Directions of Arrival of Spatially Dispersed Signals in Array Processing". *Proc. IEE Radar, Sonar and Nav.*, 143(1):1–9, Feb. 1996.

[6] R. Raich, J. Goldberg, and H. Messer. "Bearing Estimation for a Distributed Source via the Conventional Beamformer". *Proc. Stat. Signal Array Process. Workshop*, pages 5–8, Sep. 1998.

[7] M. Tapio. "Direction and Spread Estimation of Spatially Distributed Signals via The Power Azimuth Spectrum". In *Proc. IEEE ICASSP 02*, pages 3005–3008, Orlando, FL, May 2002.

[8] D. Tholl and M. Fattouche. "Angle of Arrival Analysis of Indoor Radio Propagation Channel". *Proc. Int. Conf. on Univ. Pers. Comm.*, 1:79–83, Oct. 1993.

[9] T. Trump and B. Ottersten. "Estimation of Nominal Direction of Arrival and Angular Spread using an Array of Sensors". *Signal Processing*, 50(1-2):57–69, Apr. 1996.

[10] S. Valaee, B. Champagne, and P. Kabal. "Parametric Localization of Distributed Sources". *IEEE Trans. on Signal Processing*, 43(9):2144–2153, Sept. 1995.

[11] Q. Wu and D.R. Fuhrmann. "A Parametric Method for Determining the Number of Signals in Narrow-Band Direction Finding". *IEEE Trans. on Signal Processing*, 39(8):1848–1857, Aug. 1991.

[12] P. Zetterberg. *"Mobile Cellular Communications with Base Station Antenna Arrays: Spectrum Efficiency, Algorithms and Propagation Models"*. PhD thesis, Royal Institute of Technology, Stockholm, Sweden, 1997.